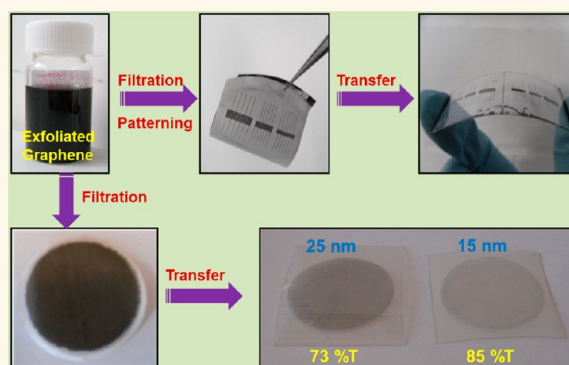


Electrochemically Exfoliated Graphene as Solution-Processable, Highly Conductive Electrodes for Organic Electronics

Khaled Parvez,[†] Rongjin Li,[†] Sreenivasa Reddy Puniredd,[†] Yenny Hernandez,[†] Felix Hinkel,[†] Suhao Wang,[†] Xinliang Feng,^{†,*,*} and Klaus Müllen^{†,*}

[†]Max Planck Institute for Polymer Research, Ackermannweg 10, D-55128 Mainz, Germany, and [‡]School of Chemistry and Chemical Engineering, Shanghai Jiao Tong University, Dongchuan Road 800, 200240, Shanghai, People's Republic of China

ABSTRACT Solution-processable thin layer graphene is an intriguing nanomaterial with tremendous potential for electronic applications. In this work, we demonstrate that electrochemical exfoliation of graphite furnishes graphene sheets of high quality. The electrochemically exfoliated graphene (EG) contains a high yield (>80%) of one- to three-layer graphene flakes with high C/O ratio of 12.3 and low sheet resistance (4.8 k Ω/\square for a single EG sheet). Due to the solution processability of EG, a vacuum filtration method in association with dry transfer is introduced to produce large-area and highly conductive graphene films on various substrates. Moreover, we demonstrate that the patterned EG can serve as high-performance source/drain electrodes for organic field-effect transistors.



KEYWORDS: electrochemical exfoliation · high-quality graphene · solution processing · organic field-effect transistors

A major challenge of organic electronics is the development of robust techniques for fabricating highly conductive, flexible, and transparent electrodes.¹ The most widely used transparent electrode is indium tin oxide (ITO), which has an optical transparency of more than 80% in the visible light range, a favorable work function (~ 4.8 eV), and a low sheet resistance of 10 to 30 Ω/\square .^{2–4} There are several limitations to ITO, however, such as sensitivity to acidic and basic environments, high surface roughness, and increasing cost due to the scarcity of indium. In addition, ITO is brittle, which leads to microcracks when the material is bent as well as dramatically reduced conductivity. Many alternative materials have been developed to replace ITO such as conducting polymers like poly(3,4-ethylenedioxythiophene):poly(styrenesulfonate) (PEDOT:PSS),⁵ carbon nanotubes (CNTs),^{6,7} metal grids, and metallic nanowires.^{8,9} Among these materials, CNT films exhibit high transparency across the visible

light spectrum, but the high resistance at the junctions between carbon nanotubes obstructs conductive pathways within the film.¹⁰

Graphene, which features high electrical conductivity, flexibility, and good mechanical and thermal stability, has emerged as a new-generation electrode material for organic electronic devices.^{11–13} Graphene-based electrodes, obtained from either solution-processed reduced graphene oxide (rGO) or graphene grown by chemical vapor deposition (CVD) methods, have been used for organic photovoltaics,¹⁴ light-emitting diodes (OLEDs),¹⁵ field-effect transistors (OFETs),^{16,17} and photodetectors.¹⁸ Electrodes prepared from rGO require chemical and/or thermal treatment of GO to partially remove the oxygen-containing groups and to restore the electrical properties. Chemical reduction by toxic hydrazine generally introduces impurities in rGO,¹⁹ while high-temperature treatment is incompatible with plastic or glass substrates. Moreover,

* Address correspondence to muellen@mpip-mainz.mpg.de; feng@mpip-mainz.mpg.de.

Received for review February 3, 2013 and accepted March 26, 2013.

Published online March 26, 2013
10.1021/nn400576v

© 2013 American Chemical Society

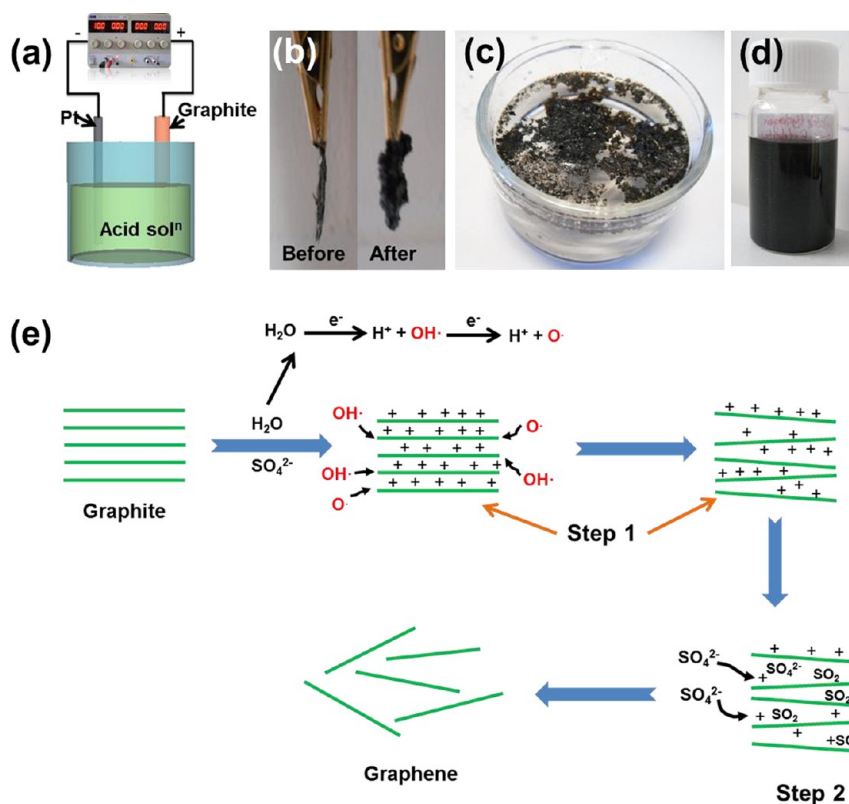


Figure 1. (a) Schematic illustration of the electrochemical exfoliation of graphite, (b) photographs of graphite flakes before and after exfoliation, (c) EG floating on top of water, (d) dispersed graphene sheets (~1 mg/mL) in DMF, and (e) schematic illustration of the proposed mechanism of electrochemical exfoliation.

high-quality graphene directly grown on Ni or Cu substrates by CVD requires a multistep transferring process involving the use of poly(methylmethacrylate) and/or polydimethylsiloxane.^{20,21} The latter are difficult to remove and may even damage the graphene film.^{22,23} Direct exfoliation of graphite in solution, such as electrochemical, sonochemical, and liquid-phase exfoliation,^{24–28} allows for the fabrication of high-quality graphene electrodes *via* a low-temperature process. Nevertheless, the yields of graphene (typically 1 to 4 layers) synthesized by these protocols remain low (<50%). In addition, due to the poor solution processability of exfoliated graphenes in high-boiling-point solvents (such as *N*-methyl-2-pyrrolidone (NMP) or *N,N'*-dimethylformamide (DMF)), it is difficult to prepare graphene films of a large area using conventional solution-processing techniques such as dip coating,¹⁴ drop casting,²⁸ spin coating,²⁹ spray casting,³⁰ inkjet printing,³¹ and Langmuir–Boldgett deposition.³² Therefore, the development of a low-cost fabrication protocol leading to highly conductive, uniform graphene films based on solution-processable graphene is highly desirable.

In the present study, we demonstrate that electrochemical exfoliation of graphite furnishes graphene sheets in high quality and high yield. The electrochemically exfoliated graphene (EG) has a large sheet size (~10 μm), low oxygen content (*i.e.*, 7.5 at. %), and low

sheet resistance (4.8 kΩ/□), which are comparable to that of CVD graphene. Due to the solution processability (~1 mg/mL in DMF) of such graphene sheets, large and homogeneous graphene films can be fabricated on both rigid and flexible substrates by vacuum filtration and subsequent transfer to the desired substrates. The resulting graphene films exhibit sheet resistances of 4.1 and 2.4 kΩ/□ with transmittances of 85% and 73%, respectively. Patterned graphene films can serve as high-performance source/drain (S/D) electrodes for OFETs.

RESULTS AND DISCUSSION

The experimental setup for electrochemical exfoliation of graphite is illustrated in Figure 1a. Typically, natural graphite flakes, platinum wires, and 0.1 M H₂SO₄ solutions were used as working electrodes, counter-electrodes, and electrolytes, respectively. When a positive voltage (*i.e.*, +10 V) was applied to a graphite electrode, the graphite flakes begin to expand, quickly dissociate, and spread into the solution (Figure 1b and c). The bias voltage was kept constant for 2 min to complete the exfoliation process. Afterward, the exfoliated graphitic material was collected by vacuum filtration and washed repeatedly with water to remove the residual acid. Finally, the obtained powder was dispersed in DMF, resulting in EG sheets (Figure 1d). The yield of EG was generally higher than 60% of the

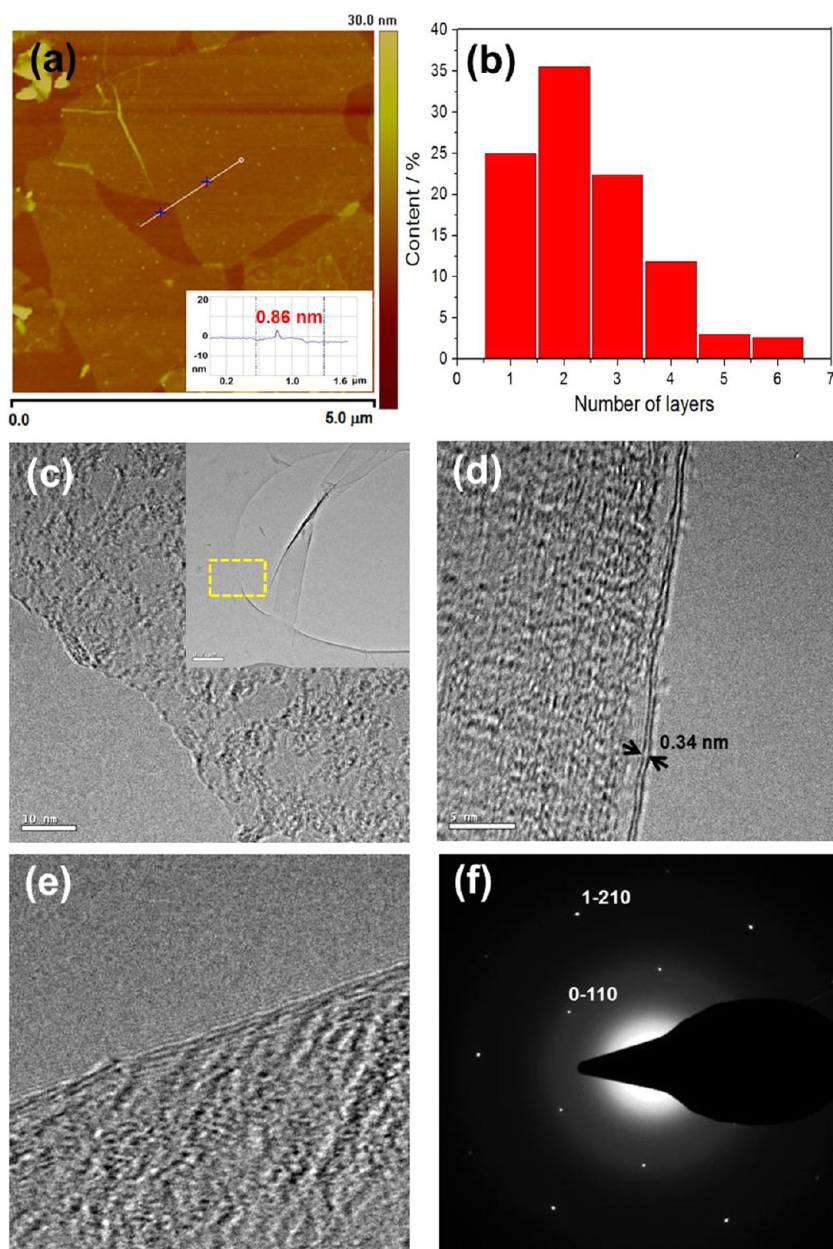


Figure 2. (a) Typical AFM image of the electrochemically exfoliated graphene on SiO_2 . (b) Statistical thickness analysis of the graphene sheets by AFM. (c, d, and e) HRTEM images of single-, bi-, and four-layer graphene. The inset in (c) is the low-magnification image of EG. To identify the number of graphene layers, the images are taken at the edge (as indicated by the dashed box). (f) SAED pattern of bilayer graphene.

total amount of starting graphite materials. Notably, a dispersion of EG with a concentration up to 1.0 mg/mL in DMF can be obtained and remains stable for several weeks without evidence of agglomeration. Moreover, the exfoliation process can be readily scaled up. By using only a ~ 2 cm long graphite electrode, more than 350 mg of EG was obtained in less than 5 min (Figure S1).

The mechanism of graphite exfoliation in 0.1 M H_2SO_4 is depicted in Figure 1e: first, applying bias voltage results in the oxidation of water, producing hydroxyl ($\text{OH}\cdot$) and oxygen radicals ($\text{O}\cdot$).³³ Oxidation or hydroxylation by these radicals initially occurs at

edge sites and grain boundaries of the graphite electrode. Second, defective sites at the edges or grain boundaries open up due to oxidation, which facilitates intercalation by anionic SO_4^{2-} . This process leads to the release of gaseous SO_2 and/or anion depolarization and causes expansion of the interlayer distance of graphite.³⁴ To understand the role of electrolytes during the exfoliation process, we have performed control experiments using H_2SO_4 with higher concentrations (1.0 and 5.0 M). The exfoliation efficiency of graphite in 1.0 and 5.0 M H_2SO_4 was much lower than that in 0.1 M H_2SO_4 , and the corresponding yield of EG was $\sim 25\%$ and $\sim 7\%$, respectively. Exfoliation in 5.0 M H_2SO_4

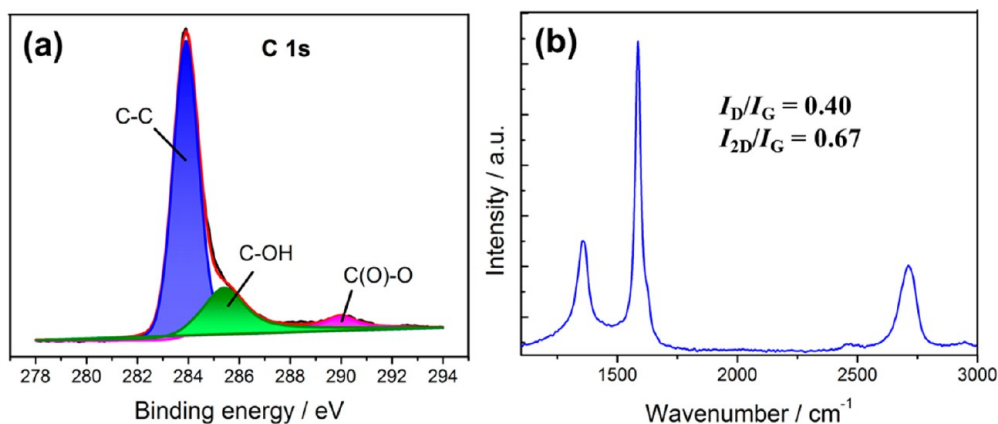


Figure 3. (a) High-resolution XPS of the C 1s peak for EG and (b) Raman spectra (excited by 488 nm laser) of a selected bilayer EG sheet. The ratios of I_D/I_G and I_{2D}/I_G peaks are indicated in the figure.

mainly generated fragments of graphite particles, which rapidly are suspended during exfoliation. Moreover, when a pure H_2SO_4 or H_2SO_4 /acetic acid mixture (1:1 ratio) was used as the electrolyte, the graphite electrode remained intact or slightly expanded due to the intercalation of negative ions when a voltage was applied for 2 h (Figure S2). These findings suggest that the presence of water in the electrolyte is crucial for the generation of oxygen or hydroxyl radicals that can react with graphite at the initial stage. When diluted H_2SO_4 (*i.e.*, 0.05 and 0.01 M) was used, however, exfoliation occurred only at a higher voltage (+12.1 and +16.0 V for 0.05 and 0.01 M, respectively) at a much lower rate (several hours were required). The EG yield for 0.05 and 0.01 M H_2SO_4 was ~34% and ~2%, respectively. The low exfoliation efficiency of EG in diluted H_2SO_4 is most likely due to the inefficient intercalation of anions into the graphite.

The morphology and number of layers in the EG sheets were first investigated by atomic force microscopy (AFM) (Figure 2a). The EG sheet was deposited on SiO_2 using the Langmuir–Blodgett (LB) technique (Figure S3a). For a typical experiment, the EG dispersion in 1:3 DMF/chloroform was added dropwise onto the water surface. A faint black-colored film was observed on the water surface after adding the EG dispersion. The film was compressed by LB trough barriers while the surface pressure was monitored using a tensiometer. Thus, EG sheets were uniformly deposited on SiO_2 by vertically dip coating the substrate, followed by thermal annealing at 200 °C to remove the residual solvent. A histogram acquired across the boundary (inset of Figure 2a) revealed a mean thickness of ~0.86 nm (Figure 2a) for monolayer graphene, which is greater than that of pristine graphene on SiO_2 (0.6 to 0.7 nm).³⁵ This result implies that a certain amount of oxygen-containing groups decorates the graphene surface. The measured thickness of bilayer graphene was ~1.5 nm (Figure S3b). The thickness distribution of 80 samples of EG sheets

calculated from the AFM height profile is shown in Figure 2b. Remarkably, more than 80% of the graphene sheets comprised one to three layers, including bilayer graphene (~35%) as a dominant product (Figure 2b). The size of the EG sheets was 5 to 10 μm , which is much larger than the size of previously reported exfoliated graphene.^{24,25,27} Transmission electron microscopy (TEM) further confirmed a mean size of ~10 μm for EG (Figure S4). High-resolution TEM (HRTEM) studies provided further support that the EG sheets ranged from a single layer up to four layers (Figure 2c to e). A typical HRTEM image of bilayer graphene with an interlayer distance of ~0.34 nm is shown in Figure 2d. Moreover, the selected area electron diffraction (SAED) pattern (Figure 2f) of the graphene sheets exhibits the typical 6-fold symmetry, consistent with the hexagonal crystalline structure of a bilayer graphene sheet.³⁶

The chemical nature of the as-prepared EG sheets was investigated by X-ray photoelectron spectroscopy (XPS). Approximately 7.5% of oxygen is present in EG, attributable to the oxidation of graphene, which was unavoidable during the electrochemical process (Figure S5). Nevertheless, a high C/O ratio of about 12.3 can be achieved for EG, in contrast to rGO (C/O ratio ~3–10) obtained by chemical or thermal reduction of GO.^{37,38} The deconvoluted XPS spectra of the C 1s peak (~284 eV) further show the presence of 5.62 at. % C–OH (285.4 eV) and 1.88% C(O)–O (290.0 eV) functional groups (Figure 3a). The Raman spectra of a bilayer EG sheet displayed an intense 2D and G peak at ~2710 and ~1586 cm^{-1} , respectively (Figure 3b). Moreover, a defect-related D peak was observed at ~1356 cm^{-1} . The intensity ratio of D to G (*i.e.*, I_D/I_G) was calculated to be 0.40. This is much lower than that of chemically or thermally reduced GO (~1.2 to 1.5).^{39,40} The intensity ratio of 2D to G (*i.e.*, I_{2D}/I_G) is normally related to the graphitization degree (for C=C sp^2 bonds) in graphitic carbons.⁴¹ The I_{2D}/I_G ratio (0.67) of bilayer EG graphene sheets produced in this work is

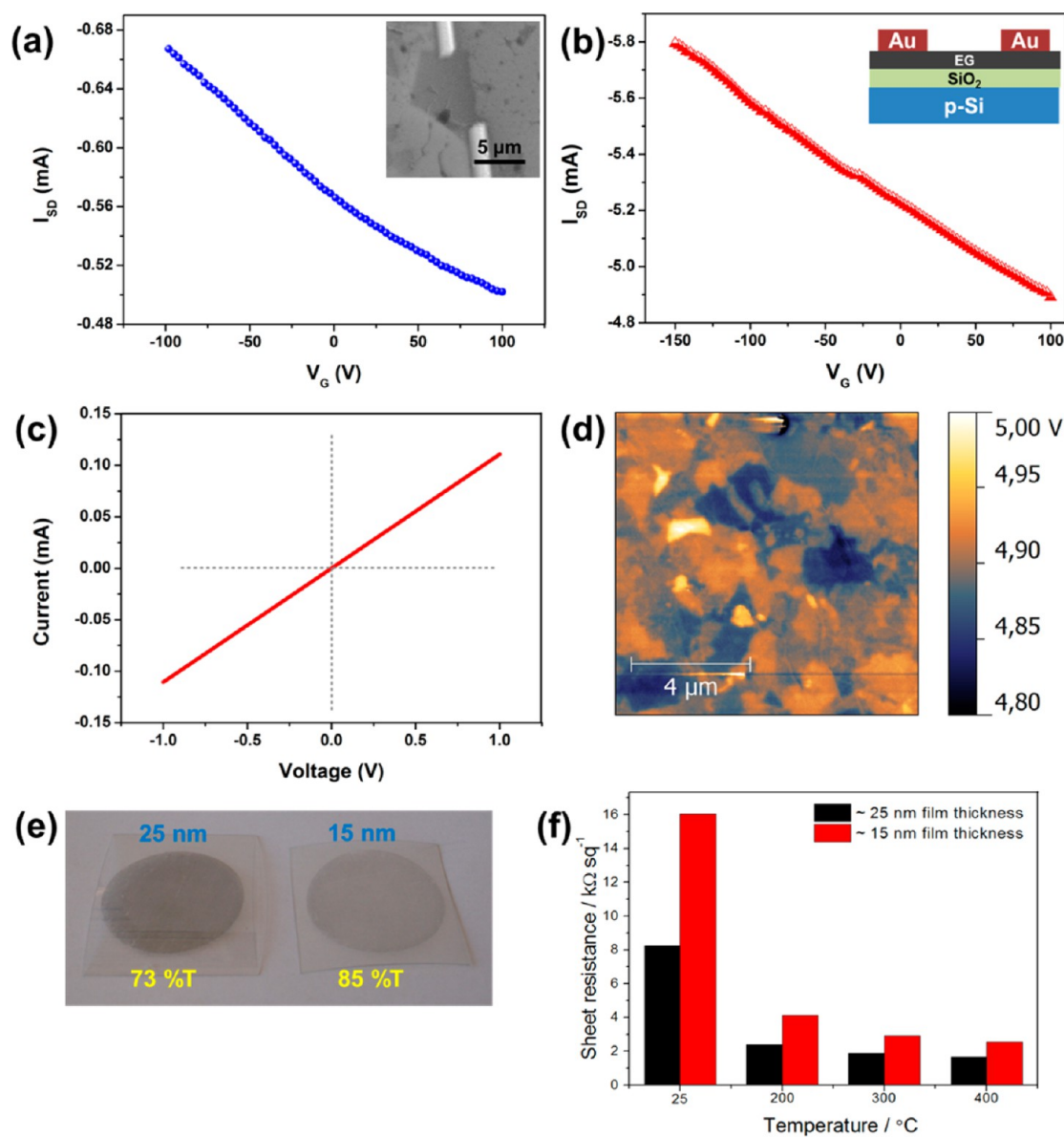


Figure 4. Transfer curve for a device prepared from (a) a bilayer EG sheet and (b) a thin EG film. Inset of (a) is an SEM image, and that of (b) is the cross-section scheme of the fabricated device. (c) Room-temperature I – V curve of a single bilayer EG sheet. (d) KPFM image showing the work function of EG. (e) Photograph of the transferred graphene film on PET substrates. (f) Sheet resistance of EG films with different thicknesses.

significantly higher than that of rGO,^{42,43} further suggesting the high quality of the EG.

The electronic properties of the resulting EG sheets were examined by bottom-gate, top-contact transistors based on a thin EG film or bilayer EG sheet. Thin-film and isolated sheets of EG on $\text{SiO}_2/\text{p-Si}$ were prepared by the LB method. The thickness of the EG film ranged from 0.8 to 3.5 nm (roughness, R_a : 1.96 nm). The transfer curves of the devices are shown in Figure 4a and b. Remarkably, the bilayer EG sheets exhibited a mean hole mobility of $\sim 233 \text{ cm}^2/(\text{V s})$, which is several times higher than that reported for electrochemically derived graphene ($5.5\text{--}17 \text{ cm}^2/(\text{V s})$)²⁸ and reduced graphene oxide ($\sim 0.01\text{--}12 \text{ cm}^2/(\text{V s})$).^{29,43–45} Moreover, the devices based on EG thin films delivered an

average mobility of $34.6 \text{ cm}^2/(\text{V s})$ with a maximum value of $47.3 \text{ cm}^2/(\text{V s})$ (Figure 4b). The lower mobility of the EG thin film compared to that of a single sheet can be attributed to the interjunction resistance between EG sheets. Further, the sheet resistance (R_s) of a single EG sheet was measured by a two-point probe system. The calculated R_s was $4.8 \text{ k}\Omega/\square$ (Figure 4c), which was much lower than that of rGO and comparable to that of CVD-grown graphene.^{46,47} The work function of EG was examined by Kelvin probe force microscopy (KPFM). A mean value of $4.90 \pm 0.05 \text{ eV}$ (Figure 4d) was obtained, which is slightly higher than that of pristine graphene ($\sim 4.6 \text{ eV}$).⁴⁸ The increased work function was due to the presence of oxygen-containing functional groups that produced surface

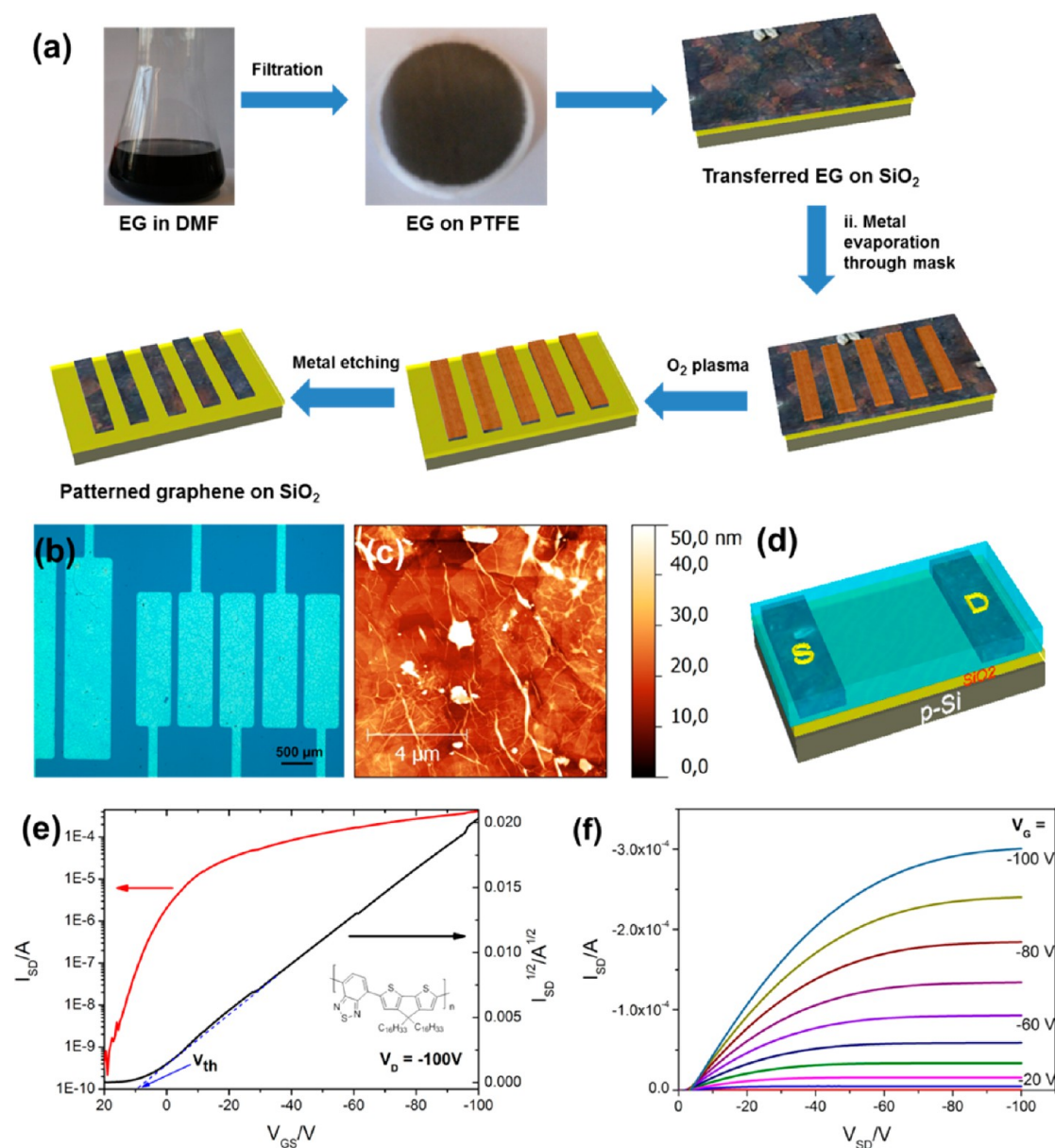


Figure 5. (a) Schematic illustration of the fabrication process of patterned EG S/D electrodes. (b) Optical image of patterned EG S/D on a SiO₂/p-Si substrate. (c) Typical AFM image of the 50 nm thick EG electrode. (d) Scheme of fabricated EG-based OFETs. (e) Transfer characteristics of the CDT-BTZ-C16-based OFETs with EG S/D electrodes ($L/W = 1/18$) at a drain bias $V_D = -100$ V. (f) Output characteristics for various gate biases V_G . The molecular structure of CDT-BTZ-C16 is shown in the inset.

$C^{\delta+}-O^{\delta-}$ dipoles *via* the extraction of π electrons from graphene.⁴⁹

The high quality and solution processability of the EG sheets led us to fabricate transparent graphene films on different substrates using a vacuum filtration and dry transfer method. To this end, an EG dispersion (~ 0.25 mg/mL) in DMF was first vacuum-filtered through a polytetrafluoroethylene (PTFE) membrane. The filtered EG film was then pressed on a target substrate such as glass or PET. When the PTFE membrane was peeled off, the EG film remained on the target substrate due to van der Waals interactions between the graphene and substrate. Unlike the vacuum filtration method, in which the filter membrane

must be dissolved in organic solvents, which may cause contamination,⁴⁵ the dry transfer method avoids dissolution of the filter membrane, which can then be reused for further experiments. Moreover, the thickness of the transferred films can be adjusted through the filtration volume and the concentration of the graphene dispersion. For example, vacuum filtration of 5 and 10 mL of EG dispersion yields ~ 15 and 25 nm graphene films on substrates, respectively. The 15 and 25 nm thick graphene films (diameter 50 mm) on PET had a transmittance of 85% and 73%, respectively (Figure 4e). It can be seen from the optical microscopic images (Figure S6) that the transferred film was uniformly covered on the substrates over a large area.

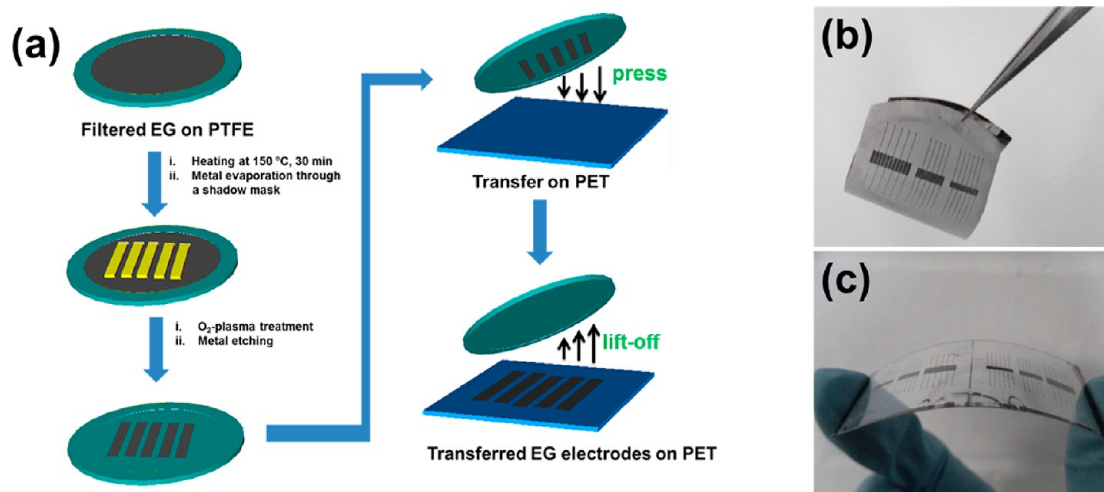


Figure 6. (a) Schematic illustration of the fabrication of patterned EG electrodes on PET substrates. (b) Photograph of EG electrodes patterned on PTFE membranes and (c) transferred on PET.

The average sheet resistance of the transferred EG films measured using the four-point probe method (Figure 4f) was 16.0 and 8.2 k Ω / \square for 15 and 25 nm EG films. Remarkably, after thermal annealing of the EG films at 200 °C for 30 min, the sheet resistance dropped dramatically to 4.1 and 2.4 k Ω / \square , respectively, attributable to the evaporation of residual DMF. Further, a simple HNO₃ (65%) treatment of 15 and 25 nm EG films significantly reduced the sheet resistance to 0.27 and 0.49 k Ω / \square , respectively (Figure S7).

The simple graphene film transfer process provides a major advantage for the solution fabrication of conductive electrodes for electronic devices. As a proof-of-concept, we demonstrated the fabrication of S/D electrodes for OFETs using patterned EG films. The fabrication process for patterned graphene electrodes from EG films is illustrated in Figure 5a (see Supporting Information for experimental details). Briefly, an EG dispersion in DMF (\sim 0.60 mg/mL) was vacuum-filtered through a PTFE membrane to obtain a 50 nm thick film and then transferred to a SiO₂/p-Si substrate by a simple mechanical press (Figure S8a). The figure shows the AFM image of a uniformly transferred EG film on a SiO₂/p-Si substrate. The conductivity of the film was 590 S/cm, which is higher than the previously reported 60 nm thick rGO S/D electrodes (500 S/cm) produced *via* thermal treatment.¹⁷ The patterned EG electrodes were obtained by thermally evaporating aluminum (Al) on top of the EG film through a mask with subsequent exposure to an O₂-plasma to remove the EG film from unmasked regions. Finally, Al was chemically etched, and EG-based S/D electrodes were generated (Figures 5b and S8b). A conjugated donor–acceptor polymer, 4*H*-cyclopenta[1,2-*b*;5,4-*b'*]dithiophenebenzo-*c*[[1,2,5]thiadiazole (CDT-BTZ-C16, M_w = 10K Da, polydispersity index = 2.67), was used as the semiconductor due to its good solution processability, close π -stacking distance, and highly ordered lamellar packing

structure on the surface.⁵⁰ The transfer and output characteristics are shown in Figure 5e and f, respectively. Remarkably, a mean hole mobility of 0.50 cm²/(V s) (maximum mobility up to 0.60 cm²/(V s)) with an on/off ratio exceeding 10⁶ was achieved. In contrast, Au-based S/D electrodes produced a mean hole mobility of only 0.19 cm²/(V s) (maximum up to 0.21 cm²/(V s)) with a lower on/off ratio (10⁵) (Figure S9a).⁵¹ For EG-based S/D devices, the desirable linear and saturation regimes with apparent gate-voltage dependence (Figure 5f) can be identified,^{52,53} in marked contrast to the S-shaped output curves derived from Au-based devices (Figure S9b). This finding strongly suggests that graphene electrodes have a low contact resistance with organic materials,⁵⁴ which is the reason for the enhanced device performance. Furthermore, flexible OFETs based on EG S/D electrodes can be fabricated on a PET substrate. In this case, the electrodes were first patterned on a filter (PTFE) membrane followed by a dry transfer process on a PET substrate (Figure 6a). S/D electrodes (\sim 50 nm thick) were fabricated on the PTFE filter by a protective metal (Al) followed by O₂-plasma etching (Figure 6a). Afterward, removal of the sacrificial Al layer in acidic solution afforded an EG film patterned on the PTFE filter (Figure 6b). Finally, the EG electrodes were transferred to a PET substrate by mechanically pressing the PTFE filter containing the patterns (Figure 6c). Thus, a top-gate OFET device was constructed by using EG electrodes patterned on PET as S/D electrodes (inset of Figure S10a). The transfer and output characteristics of a flexible OFET are shown in Figure S10, and a brief description is provided in the Supporting Information. Although the performance of a flexible OFET is inferior to the device based on the SiO₂/p-Si substrate, this study shows the potential of high-quality and solution-processable EG as electrode materials for different electronic devices.

CONCLUSION

In conclusion, the present study demonstrates that electrochemical exfoliation of graphite is a promising method for the fabrication of graphene sheets in high quality and high yield. The as-prepared graphene has a large sheet size, low oxygen content, and/or high C/O ratio as well as excellent electronic properties comparable to CVD graphene. In addition, we introduce a vacuum filtration method in association with the dry transfer method to produce highly conductive graphene films on various substrates. The high solution processability and high quality of the exfoliated graphene sheets hold enormous promise for both rigid and flexible organic electronic devices.

Conflict of Interest: The authors declare no competing financial interest.

Acknowledgment. The authors thank Dr. Shubin Yang for XPS and Haixin Zhou for HRTEM measurements. This work was financially supported by ERC grants on NANOGRAPH and 2DMATER, DFG Priority Program SPP 1459, BMBF Graphenoid Project, ESF Project GOSPEL (ref no. 09-EuroGRAPHENE-FP-001), EU Project GENIUS, and EU Project MOLESOL.

Supporting Information Available: Experimental details, AFM and TEM images and XPS spectra of EG, photograph of electrochemical exfoliation in different electrolyte systems, performance of Au electrodes and flexible EG-based OFET devices. This material is available free of charge via the Internet at <http://pubs.acs.org>.

REFERENCES AND NOTES

- Southard, A.; Sangwan, V.; Cheng, J.; Williams, E. D.; Fuhrer, M. S. Solution-Processed Single Walled Carbon Nanotube Electrodes for Organic Thin-Film Transistors. *Org. Electron.* **2009**, *10*, 1556–1561.
- Wang, X.; Zhi, L. J.; Tsao, N.; Tomovic, Z.; Li, J. L.; Müllen, K. Transparent Carbon Films as Electrodes in Organic Solar Cells. *Angew. Chem., Int. Ed.* **2008**, *47*, 2990–2992.
- Wassei, J. K.; Kaner, R. B. Graphene, A Promising Transparent Conductor. *Mater. Today* **2010**, *13*, 52–59.
- Kim, J. Y.; Lee, K.; Coates, N. E.; Moses, D.; Nguyen, T. Q.; Dante, M.; Heeger, A. J. Efficient Tandem Polymer Solar Cells Fabricated by All-Solution Processing. *Science* **2007**, *317*, 222–225.
- Na, S. I.; Kim, S. S.; Jo, J.; Kim, D. Y. Efficient and Flexible ITO-Free Organic Solar Cells Using Highly Conductive Polymer Anodes. *Adv. Mater.* **2008**, *20*, 4061–4067.
- Wu, Z. C.; Chen, Z. H.; Du, X.; Logan, J. M.; Sippel, J.; Nikolou, M.; Kamaras, K.; Reynolds, J. R.; Tanner, D. B.; Hebard, A. F.; Rinzler, A. G. Transparent, Conductive Carbon Nanotube Films. *Science* **2004**, *305*, 1273–1276.
- Rowell, M. W.; Toinka, M. A.; McGehee, M. D.; Prall, H. J.; Dennler, G.; Sariciftci, N. S.; Hu, L. B.; Gruner, G. Organic Solar Cells with Carbon Nanotube Network Electrodes. *Appl. Phys. Lett.* **2006**, *88*, 233506.
- Lee, J. Y.; Connor, S. T.; Cui, Y.; Peumans, P. Solution-Processed Metal Nanowire Mesh Transparent Electrodes. *Nano Lett.* **2008**, *8*, 689–692.
- De, S.; Higgins, T. M.; Lyons, P. E.; Doherty, E. M.; Nirmalraj, P. N.; Blau, W. J.; Boland, J. J.; Coleman, J. N. Silver Nanowire Networks as Flexible, Transparent, Conducting Films: Extremely High DC to Optical Conductivity Ratios. *ACS Nano* **2009**, *3*, 1767–1774.
- Ho, G. W.; Wee, A. T. S.; Lin, J. Electric Field-Induced Carbon Nanotube Junction Formation. *Appl. Phys. Lett.* **2001**, *79*, 260–262.
- De, S.; Coleman, J. N. Are There Fundamental Limitations on the Sheet Resistance and Transmittance of Thin Graphene Films? *ACS Nano* **2010**, *4*, 2713–2720.
- Wang, Y.; Chen, X.; Zhong, Y.; Zhu, F.; Loh, K. P. Large Area, Continuous, Few-Layered Graphene as Anodes in Organic Photovoltaic Devices. *Appl. Phys. Lett.* **2009**, *95*, 063302.
- Bae, S.; Kim, H.; Lee, Y.; Xu, X.; Park, J.-S.; Zheng, Y.; Balakrishnan, J.; Lei, T.; Kim, H. R.; Song, Y. I.; et al. Roll-to-Roll Production of 30-in. Graphene Films for Transparent Electrodes. *Nat. Nanotechnol.* **2010**, *5*, 574–578.
- Wang, X.; Zhi, L.; Müllen, K. Transparent, Conductive Graphene Electrodes for Dye-Sensitized Solar Cells. *Nano Lett.* **2008**, *8*, 323–327.
- Matyba, P.; Yamaguchi, H.; Eda, G.; Chhowalla, M.; Edman, L.; Robinson, N. D. Graphene and Mobile Ions: The Key to All-Plastic, Solution-Processed Light-Emitting Devices. *ACS Nano* **2010**, *4*, 637–642.
- Liu, W.; Jackson, B. L.; Zhu, J.; Miao, C. Q.; Heui, C.; Chung, C. H.; Park, Y. J.; Sun, K.; Woo, J.; Xie, Y.-H. Large Scale Pattern Graphene Electrode for High Performance in Transparent Organic Single Crystal Field-Effect Transistors. *ACS Nano* **2010**, *4*, 3927–3932.
- Pang, S.; Tsao, H. N.; Feng, X.; Müllen, K. Patterned Graphene Electrodes from Solution-Processed Graphite Oxide Films for Organic Field-Effect Transistors. *Adv. Mater.* **2009**, *21*, 1–4.
- Pang, S.; Yang, S.; Feng, X.; Müllen, K. Coplanar Asymmetrical Reduced Graphene Oxide-Titanium Electrodes for Polymer Photodetectors. *Adv. Mater.* **2012**, *24*, 1566–1570.
- Park, S.; An, J.; Piner, R. D.; An, S. J.; Li, X.; Velamakanni, A.; Rouff, R. S. Colloidal Suspensions of Highly Reduced Graphene Oxide in a Wide Variety of Organic Solvents. *Nano Lett.* **2009**, *9*, 1593–1597.
- Kim, K. S.; Zhao, Y.; Jang, H.; Lee, S. Y.; Kim, J. M.; Kim, K. S.; Ahn, J. H.; Kim, P.; Choi, J. Y.; Hong, B. H. Large-Scale Pattern Growth of Graphene Films for Stretchable Transparent Electrodes. *Nature* **2009**, *457*, 706–710.
- Lee, Y.; Bae, S.; Jang, H.; Jang, S.; Zhu, S. E.; Sim, S. H.; Song, Y. I.; Hong, B. H.; Ahn, J. H. Wafer-Scale Synthesis and Transfer of Graphene Films. *Nano Lett.* **2010**, *10*, 490–493.
- He, M.; Jung, J.; Qiu, F.; Lin, Z. Q. Graphene-Based Transparent Flexible Electrodes for Polymer Solar Cells. *J. Mater. Chem.* **2012**, *22*, 24254–24264.
- Pirkle, A.; Chan, J.; Venugopal, A.; Hinojos, D.; Magnuson, W. C.; McDonnell, S.; Colomobo, L.; Vogel, E. M.; Ruoff, R. S.; Wallace, R. M. The Effect of Chemical Residues on the Physical and Electrical Properties of Chemical Vapor Deposited Graphene Transferred to SiO₂. *Appl. Phys. Lett.* **2011**, *99*, 122108.
- Liu, N.; Luo, F.; Wu, H.; Liu, Y.; Zhang, C.; Chen, J. One-Step Ionic-Liquid Assisted Electrochemical Synthesis of Ionic-Liquid-Functionalized Graphene Sheets Directly from Graphite. *Adv. Funct. Mater.* **2008**, *18*, 1518–1525.
- Wang, J.; Manga, K. K.; Bao, Q.; Loh, K. P. High-Yield Synthesis of Few-Layer Graphene Flakes through Electrochemical Expansion of Graphite in Propylene Carbonate Electrolyte. *J. Am. Chem. Soc.* **2011**, *133*, 8888–8891.
- Xu, H.; Suslick, K. S. Sonochemical Preparation of Functionalized Graphenes. *J. Am. Chem. Soc.* **2011**, *133*, 9148–9151.
- Hernandez, Y.; Nicolosi, V.; Loyta, M.; Blighe, F. M.; Sun, Z.; De, S.; McGovern, I. T.; Holland, B.; Byrne, M.; Gun'ko, Y. K.; et al. High-Yield Production of Graphene by Liquid-Phase Exfoliation of Graphite. *Nat. Nanotechnol.* **2008**, *3*, 563–568.
- Su, C. Y.; Lu, A. Y.; Xu, Y.; Chen, F. R.; Khlobystov, A. N.; Li, L. J. High-Quality Thin Graphene Films from Fast Electrochemical Exfoliation. *ACS Nano* **2011**, *5*, 2332–2339.
- Tung, V. C.; Allen, M. J.; Yang, Y.; Kaner, R. B. High-Throughput Solution Processing of Large-Scale Graphene. *Nat. Nanotechnol.* **2008**, *4*, 25–29.
- Gilje, S.; Han, S.; Wang, M.; Wang, K. L.; Kaner, R. B. A Chemical Route to Graphene for Device Applications. *Nano Lett.* **2007**, *7*, 3394–3398.
- Shin, K. Y.; Hong, J. Y.; Jang, J. Flexible and Transparent Graphene Films as Acoustic Actuator Electrodes Using Inkjet Printing. *Chem. Commun.* **2011**, *47*, 8527–8529.

32. Li, X.; Zhang, G.; Bai, X.; Sun, X.; Wang, X.; Wang, E.; Dai, H. Highly Conducting Graphene Sheets and Langmuir-Blodgett Films. *Nat. Nanotechnol.* **2008**, *3*, 538–542.
33. Lu, J.; Yang, J. X.; Wang, J.; Lim, A.; Wang, S.; Loh, K. P. One-Pot Synthesis of Fluorescent Carbon Nanoribbons, Nanoparticles, and Graphene by the Exfoliation of Graphite in Ionic Liquids. *ACS Nano* **2009**, *3*, 2367–2375.
34. Kang, F.; Leng, Y.; Zhang, T. Y. Influences of H₂O₂ on Synthesis of H₂SO₄-GICs. *J. Phys. Chem. Solids* **1996**, *57*, 889–892.
35. Cheng, Z. G.; Zhou, Q. Y.; Wang, C. X.; Li, Q. A.; Wang, C.; Fang, Y. Toward Intrinsic Graphene Surfaces: A Systematic Study on Thermal Annealing and Wet-Chemical Treatment of SiO₂-Supported Graphene Devices. *Nano Lett.* **2011**, *11*, 767–771.
36. Sun, Z.; Yan, Z.; Beitler, E.; Zhu, Y.; Tour, J. M. Growth of Graphene from Solid Carbon Sources. *Nature* **2010**, *468*, 549–552.
37. Compton, O. C.; Jain, B.; Dikin, D. A.; Abouimrane, A.; Amine, K.; Nguyen, S. T. Chemically Active Reduced Graphene Oxide with Tunable C/O Ratios. *ACS Nano* **2011**, *5*, 4380–4391.
38. Park, S.; Rouff, R. S. Chemical Methods for Production of Graphenes. *Nat. Nanotechnol.* **2009**, *4*, 217–224.
39. Mattevi, C.; Eda, G.; Agnoli, S.; Miller, S.; Mkhoyan, K. A.; Celik, O.; Mastrogianni, D.; Granozzi, G.; Garfunkel, E.; Chhowalla, M. Evolution of Electrical, Chemical, and Structural Properties of Transparent and Conducting Chemically Derived Graphene Thin Films. *Adv. Funct. Mater.* **2009**, *19*, 2577–2583.
40. López, V.; Sundaram, R. S.; Navarro, C. G.; Olea, D.; Burghard, M.; Herrero, J. G.; Zamora, F.; Kern, K. Chemical Vapor Deposition of Graphene Oxide: A Route to Highly-Conductive Graphene Monolayers. *Adv. Mater.* **2009**, *21*, 4683–4686.
41. Krauss, B.; Lohmann, T.; Chae, D. H.; Haluska, M.; Klitzing, K. V.; Smet, J. H. Laser-Induced Disassembly of a Graphene Single Crystal into a Nanocrystalline Network. *Phys. Rev. B* **2009**, *79*, 165428.
42. Zhao, F.; Liu, J.; Huang, X.; Zou, X.; Lu, G.; Sun, P.; Wu, S.; Ai, W.; Yi, M.; Qi, X.; *et al.* Chemoselective Photodeoxidation of Graphene Oxide Using Sterically Hindered Amine as Catalyst: Synthesis and Applications. *ACS Nano* **2012**, *4*, 3027–3033.
43. Su, C. Y.; Xu, Y.; Zhang, W.; Zhao, J.; Tang, X.; Tsai, C. H.; Li, L. J. Electrical and Spectroscopic Characterizations of Ultra-Large Reduced Graphene Oxide Monolayers. *Chem. Mater.* **2009**, *21*, 5674–5680.
44. Su, C.; Xu, Y.; Zhang, W.; Zhao, J.; Liu, A.; Tang, Z.; Tsai, C. H.; Huang, Y.; Li, L. Highly Efficient Restoration of Graphitic Structure in Graphene Oxide Using Alcohol Vapors. *ACS Nano* **2010**, *4*, 5285–5292.
45. Eda, G.; Fanchini, G.; Chhowalla, M. Large-Area Ultrathin Films of Reduced Graphene Oxide as a Transparent and Flexible Electronic Material. *Nat. Nanotechnol.* **2008**, *3*, 270–274.
46. Reina, A.; Jia, X. T.; Ho, J.; Nezich, D.; Son, H. B.; Bulovic, V. Large Area, Few-Layer Graphene Films on Arbitrary Substrates by Chemical Vapor Deposition. *Nano Lett.* **2009**, *9*, 30–35.
47. Shi, Z.; Yang, R.; Zhang, L.; Wang, Y.; Liu, D.; Shi, D. Patterning Graphene with Zigzag Edges by Self-Aligned Anisotropic Etching. *Adv. Mater.* **2011**, *23*, 3061–3065.
48. Yu, Y. J.; Zhao, Y.; Ryu, S.; Brus, L. E.; Kim, K. S.; Kim, P. Tuning the Graphene Work Function by Electric Field Effect. *Nano Lett.* **2009**, *9*, 3430–3434.
49. Li, S. S.; Tu, K. H.; Lin, C. C.; Chen, C. W.; Chhowalla, M. Solution-Processable Graphene Oxide as an Efficient Hole Transport Layer in Polymer Solar Cells. *ACS Nano* **2010**, *4*, 3169–3174.
50. Tsao, H. N.; Cho, D. M.; Park, I.; Hansen, M. R.; Mavrinsky, A.; Yoon, D. Y.; Graf, R.; Pisula, W.; Spiess, H. W.; Müllen, K. Ultrahigh Mobility in Polymer Field-Effect Transistor by Design. *J. Am. Chem. Soc.* **2011**, *133*, 2605–2612.
51. Zhang, M.; Tsao, H. N.; Pisula, W.; Yang, C.; Mishra, A. K.; Müllen, K. Field-Effect Transistors Based on a Benzothiadiazole-Cyclopentadithiophene Copolymer. *J. Am. Chem. Soc.* **2007**, *129*, 3472–3473.
52. Moore, V. C.; Strano, M. S.; Haroz, E. H.; Hauge, R. H.; Smalley, R. E.; Schmidt, J.; Talmon, Y. Individually Suspended Single-Walled Carbon Nanotubes in Various Surfactants. *Nano Lett.* **2003**, *3*, 1379–1382.
53. Navarro, C. G.; Weitz, R. T.; Bittner, A. M.; Scolari, M.; Mewa, A.; Burghard, M.; Kern, K. Electronic Transport Properties of Individual Chemically Reduced Graphene Oxide Sheets. *Nano Lett.* **2007**, *7*, 3499–3503.
54. Di, C. A.; Wei, D.; Yu, G.; Liu, Y.; Guo, Y.; Zhu, D. Patterned Graphene as Source/Drain Electrodes for Bottom-Contact Organic Field-Effect Transistors. *Adv. Mater.* **2008**, *20*, 3289–3293.